

Inversion of Surface Displacements to Monitor *In Situ* Processes

MAURICE B. DUSSEAULT†
 ROMAN A. BILAK†
 LEO ROTHENBURG†

INTRODUCTION

Enhanced Oil Recovery (EOR) processes often involve injection and production of large volumes of fluid. The engineer wants to know where injected fluids are going, and where produced fluids are coming from; this requires monitoring. Pressure-volume-temperature data may be collected, observation wells drilled and instrumented, periodic geophysical logging performed, 3-D seismic surveys carried out, and so on. However, some approaches are costly and require many wells, others give data at a single point or with little spatial resolution, yet others are difficult to interpret in terms of parameters that the reservoir engineer can use.

EOR processes involve large stress and temperature changes, which lead to deformations. These create a three-dimensional displacement field which can in principle be measured and analyzed to give process information. Thus, remote displacement monitoring is an appealing monitoring concept, providing data can be related to process evolution. This article describes such an approach, along with a case history.

THE PHYSICAL MODEL

A zone of volume change (ΔV) or shear deformation (ΔS) at depth affects the entire continuum; remote displacements (Fig. 1) are functions of magnitude, size and distance, and are only weakly dependent on elastic properties because remote motions are dominated by translational displacements rather than local straining. To quantify ΔV and ΔS from measurements, enough data points of high precision from a coherent displacement field must be collected and analyzed. For remote monitoring of the displacement field arising from injection or production of fluids, it is reasonable to treat the overburden as an elastic body, as it experiences only small strains, on the order of 10^{-4} and less [1]. Also, in the reservoir, no large metastable cavities exist, as in mining and solution cavity cases. All ΔV and ΔS show up in the displacement field, whether deformations are irreversible or otherwise.

Mathematically, using displacements to solve for ΔV and ΔS at depth is called "inversion". Numerically, it is done by subdividing the domain and distributing deformations over a number of "source functions", each equivalent to a kernel of an integral operator equation [2].

If sources are small relative to depth, movements are expressed as the sum of displacements from each source. Thus, for a surface array ($Z=0$):

$$U_z(r') = \int_V U^*(r', r) E_v(r) dV(r); \text{ or:} \quad (1)$$

$$\Delta x, \Delta y, \Delta z]_{x,y,z=0} = \sum_{i=1}^N \Delta x_i K(u_i, v_i, w_i), \Delta y_i K...$$

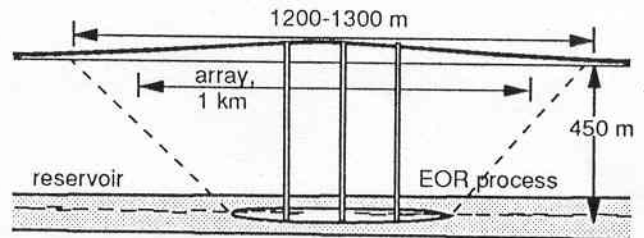


Fig. 1: Reservoir Strains Transmitted to Surface

Stated in words: if a Green's Function U^* uniquely relates volume change E_v in any volumetric element in the half space to surface displacements, $U_z(r')$ at $(X,Y,Z=0)$, then $(\Delta x, \Delta y, \Delta z)_{z=0}$ is the sum of individual contributions from each source. In (1), there are N unique ΔV point sources contributing to $\Delta x, \Delta y, \Delta z$ at each surface point. K (the kernel) is in closed-form for some cases, one of which leads to nucleus-of-strain approaches where displacements are solved in terms of $\{\Delta V\}$ only [3,7]. Inverting (1) can be done directly, but only after problems of ill-conditioning are recognised and handled [4,5,6]. Ill-conditioning leads to different and chaotic solutions for minor differences in data, but developments referred to as "regularizations" [5], permit solutions to be extracted from noisy data and ill-conditioned cases.

Finite element analysis can be used to derive a numerical value for K , hence solutions are not constrained to closed-form kernel cases. Limited heterogeneity and anisotropy [1] can thus be treated, with numerical influence functions used directly in the equations.

For a nucleus-of-strain formulation, the summation in (1), using only $\{\Delta z\}$, leads to:

$$\{\Delta z\}_{z=0} = [a_{i,j}] \{\Delta V\} \quad (2)$$

where volume change $\{\Delta V\}$ is sought, and $[a_{i,j}]$ is a full matrix which must be inverted to solve the problem.

The nucleus-of-strain approach [7] does not allow ΔS distributions to be inferred; for this, a displacement discontinuity approach is used [8]. The reservoir is

†Terralog Technologies Incorporated, #900, 840-7th Ave. SW, Calgary, Alberta, CANADA, T2P 3G2

represented by 10 variables: location (x, y, z), dip and dip direction (ϕ, Θ), area (W, L), and planar displacements ($\delta u, \delta v, \delta w$). A forward solution exists for such a plane at any orientation [8], and predictions are compared with surface data using classical forward optimisation methods such as least-squares minimisation [4], but the solution is constrained by knowledge of the stratigraphy, well locations, and so on. Results are interpreted as spatially averaged measures, and, as with all monitoring inversions, the solution is considered the most probable one. FEM solutions are often considered as "precise results", despite uncertainty in behaviour and geometry, whereas inversions are considered imprecise because real measurements always have errors. Given the choice, we prefer analyzing real data.

Elastic overburden assumptions are often questioned because of large ΔV and ΔS . Extensive modelling and field verification of subsidence and uplift confirm the validity of these assumptions; not only are strains small, but displacements in the reservoir are transmitted effectively to the surface as translational movements rather than strains, whether the overburden is stiff or soft [1]. Furthermore, because analysis is of Δz differences, not absolute values, the overburden likely behaves in an identical manner between surveys. Reservoir strains are obviously non-elastic, and plastic deformation details cannot be resolved by remote techniques, a concept known in continuum mechanics (d'Alembert's Principle). A number of cases have been analyzed, showing elastic assumptions to be valid and inversions to be consistent, meaningful, and useful. Validations include volumetric balance, production correlations, realized well casing shear predictions, and spatial correlations, as demonstrated in this paper. Results are treated as spatial averages, rather than as precise punctual predictions.

To achieve a solution, constraints are necessary; data must not be smoothed or contoured, and the number of variables must be less than the number of reliable data points. Local minima in optimization space must be avoided, and repeated solutions are necessary, with the operator applying intelligent input to the process. In each project, as more is learned about the system response with subsequent analyses, and interpretations become progressively better and more useful.

THE FIELD APPROACH

The surface displacement field is sampled accurately; 12-40 points are needed if tiltmeters are used in a simple project, 100-500 points if Δz is used over a large area. Vertical displacements $\{\Delta z\}$ from precision levelling, tilt vectors $\{\delta\Theta, \delta\Omega\}$ from tiltmeters [9], or lateral displacements $\{\Delta x, \Delta y\}$ from precise laser ranging are acceptable. Generally, first-order geodetic levelling approaches are used with submillimetre accuracy over 100 m. Tiltmeters giving submicroradian accuracy, an order of magnitude more accurate than levelling but more costly to obtain, are also used. Geometry depends on monitoring goals, project size and depth, and desired accuracy. The array is designed with forward numerical models, analyzing various scenarios to study the layout carefully. Typically, a reservoir deformation field ($\Delta V_i, \Delta S_i$) is

assumed, $\{\Delta z\}$ or $\{\delta\Theta, \delta\Omega\}$ data generated by sampling the predicted surface displacement field at 50 to 400 points, and the data are perturbed in various ways, artificially introducing random error. Perturbed data are mathematically analyzed, and solutions statistically compared with the initial source parameters, $\Delta V_i, \Delta S_i$, used to generate the data. These scenario studies are well known in inversion and analysis, particularly in geophysics [4]; they indicate sampling points number, spacing, and survey accuracy required to achieve a particular analysis accuracy.

For most projects, a survey each 3 to 8 weeks suffices. It is best to survey before a change of activity, such as a major injection cycle, then resurvey after the event, analyzing only the changes. This reduces analysis size, and allows incorporation of constraints which facilitate mathematical treatment. Survey precision must high; ± 0.7 mm precision can be achieved systematically over baselines of 100 m, permitting analysis of displacement fields as small as 7 mm average. To achieve survey repeatability, deeply anchored benchmarks are used so that moisture and temperature changes have little effect. Installation depth can vary from 3 m to 20 m. Some random error can be tolerated, but systematic error, if undetected or uncorrectable, leads to well-known inversion and interpretation difficulties [4,5].

A FIELD CASE

Twenty-five wells were drilled into a 31% porosity, 30 m thick, heavy oil reservoir at -450 m in Alberta to test cyclic steam stimulation. Rows were steamed with 300 m³/day/well for 25 days, using row-by-row 60% overlapping injection. As steaming moved to new rows, each freshly steamed row was shut-in to soak for a few days, placed on flowback, then pumped. When steaming reached the top, the process was repeated starting at the bottom, with a full cycle taking about 20-25 weeks. The operator wanted to understand fluid retention patterns, mechanics of formation behaviour, where production was occurring, if recompaction was important, and so on.

Before steaming, the project was instrumented with benchmarks at 5 m depth, and the array was sufficiently dense (186 points, Fig. 2) to allow detailed ΔV and ΔS analysis. First-order geodetic surveying was used, usually after two rows of steaming (5 weeks), and the array was closed over a two-day period to no more than 2-3 mm. Corrections were made to reduce error at single benchmarks to ± 0.7 mm, based on local resurveying to assess consistency. There were no known sources of systematic error, seasonal benchmark stability was excellent, and the nature of the overburden response never varied.

Benchmark elevation differences, $\{z_{i+\Delta t} - z_i\}$, for selected cross-sections at a particular time are shown in Fig. 3. Dots are real data; solid lines represent values of the best reconstruction using the forward model, once the optimisation method had been used to compute the best-fit displacement discontinuity planes. Typically, $\{\Delta z\}$ values were from 10 to 40 mm above injection wells, and in the rows on flowback and initial production, subsidence was as much as 14 mm. Thus, about $\frac{1}{3}$ of the vertical

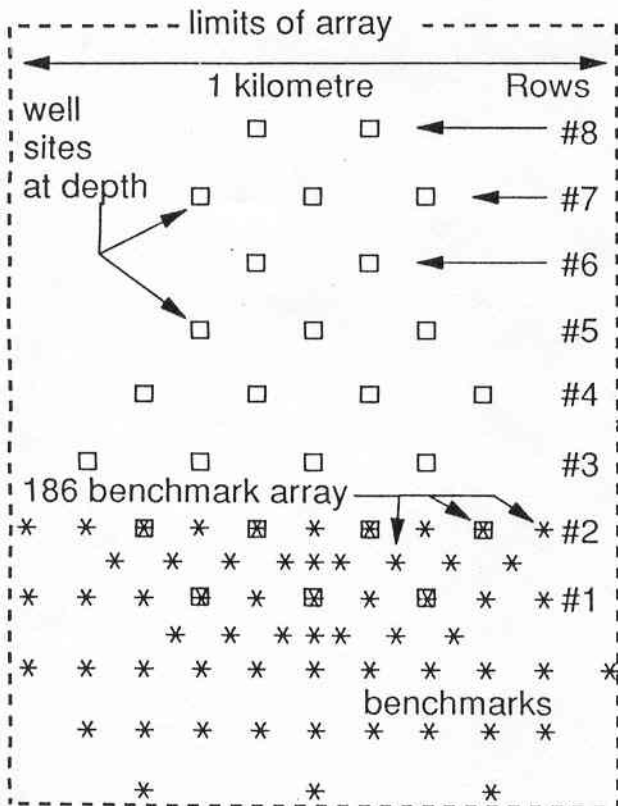


Fig. 2. Benchmark and Well Layout

movements were recovered during 1st cycle production. The good correlation of the results to production data and well location over 8 surveys during a 14-month period confirm that assumptions of elastic overburden behaviour are justified, and that surface displacements faithfully reflect deep processes.

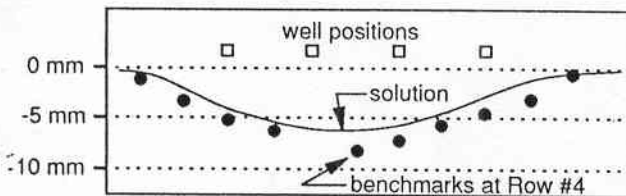


Fig. 3: Typical Data and Solution Curve

Fig. 4 is one reconstruction using the displacement discontinuity plane approach, with the overburden treated as a horizontally stratified but elastic medium. Well rows are labelled IC for injection cycle, FB for flowback, and PC for production cycle. From the top down, over the September-October period, Row #8 was dominated by 1st cycle injection, Row #7 was converted from injection to flowback without artificial lift, Row #6 was on flowback, then lift was established, Rows #5, #4, and #3 were only on lift; Row #2 was inactive, being prepared for second cycle steaming; and, towards the end of the period, Row #1 was placed on the second steam injection cycle.

As part of the analysis, a nucleus-of-strain inversion [3,4,7] was also used, but it does not solve for $\{\Delta S\}$, only $\{\Delta V\}$; nevertheless, $\{\Delta V\}$ spatially correlates well with the deformation plane solution, as expected. On Fig. 4, the surface trace of zero reservoir ΔV is shown; it falls cleanly

between the two groups of planes.

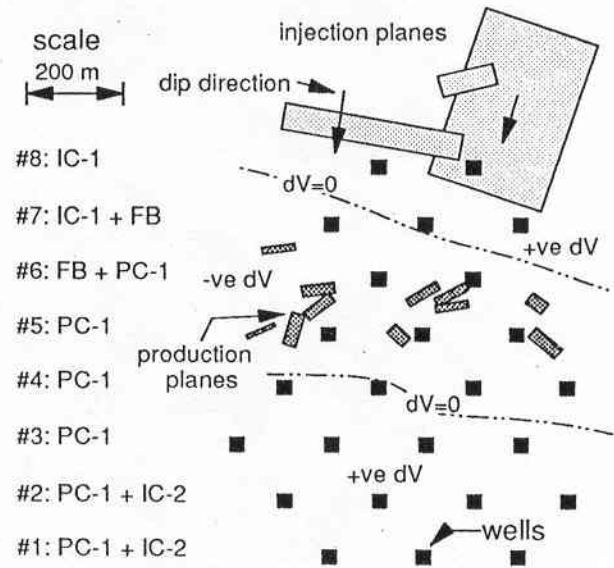


Fig. 4. Deformation Zone Reconstruction

The large planes represent the best-fit aggregate deformation from injection into the top 2 rows; most went into the top row. Each plane has slip (ΔS) along it, as much as 35 mm average; the sense of motion is thrust at low angles (6-15°), with the top moving upwards on the diagram, but the dip direction in the opposite sense. ΔS is related to horizontal total stress (σ_h) increase and reduction in effective stresses (σ') because of high pressure injection [10]. Steam was injected under back-calculated bottomhole pressures $\approx 1.15\sigma_v$, indicating horizontal fracturing. This corresponds to $\sigma_v = \sigma_3$, with $\sigma_{hmax} = \sigma_1$ at an angle of 15-20° clockwise from the project axis. The large 1st cycle shear slips reflect initial *in situ* stresses; in this region, σ_{hmax} is approximately aligned with the large slip plane dip direction. Initially, $\sigma_3 = \sigma_{hmin}$, but soon after injection began, principal stress direction rotation occurred, and σ_3 became σ_v , evidenced by the sub-horizontal deformation planes. In subsequent cycles, virgin stress effects disappeared; response was dominated by stresses induced by large injection volumes and high temperatures.[10] It has been noted here and in other projects that ΔS is largest in 1st cycles, and decays to small values in subsequent cycles.

The small dark planes around Rows #5 and #6 are reconstructed recompaction planes. Initial stiffness is high ($\approx 10^6 \text{ kPa}^{-1}$), so little compaction occurs during depletion, thus recompaction planes indicate dilation during injection, about 1/3 of which is recoverable. This fraction rises in later cycles until, after 5-6 cycles, uplift corresponds to subsidence, but with much initial uplift remaining as dilation in these dense sands is never fully recovered. Recompaction planes have appreciable $-\Delta V$, but there is almost no ΔS ; compaction is purely volumetric as pore pressure reductions increase σ'_v across the planes, preventing slip. There are no detectable volumetric strains in the four lower rows, despite continued fluid production in Rows #4 and #3. These are producing mostly water, whereas rows that display compaction produce appreciable oil. This remarkable and unexpected finding confirms

recompaction as a drive mechanism as early as the 1st cycle of production; evidently, large volumes of the reservoir are "fluffed-up", and recompaction helps oil recovery.

SUMMARY OF EOR-RELATED FINDINGS

To date, several cyclic steam injection projects at various depths and using various technologies for injection and production have been monitored using surface displacements. A consistent picture of rock mechanics behaviour is emerging, and some important generalizations can be made:

1. 1st cycle injection generates large ΔS fields, which can shear well casings and cause reservoir seal impairment. ΔS magnitude decreases in later cycles, when displacements are dominated by volumetric dilation.

2. Production cycles are ΔV -dominated; little shear can be reconstructed. In initial cycles, 30-40% of ΔV is recovered as recompaction; this rises towards 100% in later cycles, with considerable permanent volume increase.

3. Oil production is related to recompaction; when recompaction ceases, oil production rates drop off rapidly.

4. During 1st cycle, ΔS and ΔV geometry are strongly affected by *in situ* stresses; in second and subsequent cycles, they reflect process-induced, not virgin stresses.

CONCLUSIONS

Surface displacements above underground EOR activity can be analyzed in terms of volume changes and shear displacements. The analytical procedure uses mathematical treatment of ill-conditioned problems, forward optimization, numerical kernel functions, and must also incorporate constraints arising from process knowledge, geology, and evolution of the analyses from period to period. The approach is applicable to all surface displacement problems related to fluid or ore extraction, providing the overburden is behaving as a continuum, rather than caving. Continuous monitoring gives insight to

process physics and progress, and may provide a means of effective process control.

REFERENCES

1. Gambolati, G., Gatto, P., Ricceri, G. Land subsidence due to gas-oil removal in layered anisotropic soils by a finite element method. In: Land Subsidence; Proc. 3rd Int. Symp. on Land Subsidence, Venice, Italy, 29-41, 1984.
2. Butkovskiy, A.G. Green's Functions and Transfer Functions Handbook, Ellis Horwood Ltd., Chichester, 237 p., 1982.
3. Geertsma, J. A Numerical Technique for Predicting Subsidence Above Compacting Reservoirs, Based on the Nucleus-of-Strain Concept. Verh. Kon. Ned. Geol. Mijnbouwkundig Genootschap, Vol 28, 43-62, 1973.
4. Menke, W. Geophysical Data Analysis: Discrete Inverse Theory. Int. Geophys. Series, Vol. 45, Academic Press, San Diego, 1989.
5. Tikhonov, A.N. and Arsenin, V.Y. Solution of Ill-Posed Problems. V.H. Winston & Sons, Washington.
6. Bilak, R.A. 1989. Analysis of Surface Deformation above Hydrocarbon Producing Reservoirs. MSc Thesis, Dept. of Earth Sciences, U. of Waterloo, 185 pp.
7. Mindlin R.D. and Cheng, D.H. Nuclei of Strain in the Semi-Infinite Solid. J. of Appl. Physics, 21, 1950.
8. Okada, Y. Surface deformation due to shear and tensile faults in a half-space. Bull. of the Seismological Society of America, 75, 4, 1135-1154, 1985.
9. Davis, P.M. Surface deformation associated with a dipping hydrofracture, Jour. of Geophysical Research, 88(B7), 5826-5834, 1983.
10. Dusseault, M.B. Stress Changes in Thermal Operations. Proc. 1993 Inter. Thermal Operations Symp., Bakersfield, CA, 319-329, Paper SPE 25809.